Spectrophotometric and Calorimetric Studies on Nickel(II) Chloro Complexes in Acetonitrile

Honoh SUZUKI and Shin-ichi ISHIGURO*
Department of Electronic Chemistry, Tokyo Institute of Technology at Nagatsuta, 4259 Nagatsuta, Midori-ku, Yokohama 227

(Received June 22, 1992)

Complexation equilibria between nickel(II) and chloride ions have been studied in acetonitrile (MeCN) by spectrophotometry and calorimetry at 25°C. Formation of four mononuclear complexes, $[Ni^{II}Cl_n]^{(2-n)+}$ ($n=1$—4), has been found, and their formation constants, enthalpies and entropies have been determined. Individual electronic spectra of the complexes are obtained for both charge-transfer (CT) bands (230—350 nm) and d-d transition bands(320—840 nm). These spectra indicate coordination geometries of octahedral complexes {$[Ni(MeCN)_6]^{2+}$, $[NiCl(MeCN)_5]^+$, $[NiCl_2(MeCN)_4]$} and tetrahedral ones {$[NiCl_3(MeCN)]^-$, $[NiCl_4]^{2-}$}. The tetrachloronickelate (II) complex is less stable and the overall formation is more endothermic than the analogous copper(II) and zinc(II) complexes. For these metal systems, the overall complexation reactions are more favored and more exothermic in MeCN than in *N,N*-dimethylformamide (DMF), which is ascribed to the much weaker solvation toward hard metal ions in MeCN.

Acetonitrile (MeCN) is a versatile aprotic solvent for organic syntheses and electrochemical studies. It has a medial dielectric constant (35.9)[1] which makes it a good solvent for electrolytes, but has only modest solvating power toward anions and hard cations, as can be expected from its relatively small donor and acceptor numbers ($D_N=14.1$, $A_N=19.3$).[2] Consequently, many solutes have high and differentiated reactivities in MeCN. Indeed, formation of copper(II) chloro complexes is extensively enhanced and more exothermic in MeCN[3] than in *N,N*-dimethylformamide (DMF),[4] which is attributable to the smaller solvation energy of Cu^{2+} in MeCN. Persson et al. recently reported a study on zinc(II) and mercury(II) halide complexes in MeCN, in which they also pointed out the importance of the tendency of MeCN to interact specifically with soft cations.[5] In this regard, however, the highly-polarizable nitrogen donor atom of MeCN might behave differently from that of the oxygen donor atom of DMF, even toward hard cations. For example, the ligand field strength of MeCN is appreciably larger than that of DMF, which may influence the ligand field energies of solvated transition metal ions. To clarify this point, it is essential to compare solution equilibria of various transition metal ions in MeCN and in DMF.

In this paper, we present a study on nickel(II) chloro complexes in MeCN. Although there are many equilibrium studies in MeCN,[6] few thermodynamic quantities are available for this system. The results are compared with those for other metal ions and those in DMF, which allows us to interpret the structures and stabilities of the complexes in terms of solvation energies and ligand field stabilization energies.

Experimental

Reagents. Reagent-grade chemicals were used. *Nickel(II) tetrafluoroborate MeCN solvate* was prepared by oxidizing nickel foil with nitrosyl tetrafluoroborate in MeCN under reduced pressure, and recrystallized from MeCN/ethyl acetate under nitrogen atmosphere.[7,8] The obtained solvate was finally stored as a stock solution in MeCN, and the metal concentration was determined by EDTA titrations with Cu-PAN indicator.[9] *Tetraethylammonium tetrafluoroborate* was prepared and purified according to the literature.[10] Other chemicals were purified as described earlier.[4] All solutions were prepared and stored in a dry box over P_2O_5.

Measurements. Test solutions contained 0.2 mol dm^{-3} $(C_2H_5)_4NBF_4$ as a constant ionic medium. Electronic spectra were measured at (25.0±0.1)°C with a quartz flow cell, which was connected to a titration vessel through Teflon tubes and a circulating Teflon pump. An $Ni(BF_4)_2$ solution was titrated with a $(C_2H_5)_4NCl$ solution under nitrogen atmosphere, and absorbances were recorded with a spectrophotometer 340 (Hitachi) equipped with a microcomputer PC9801VM2 (NEC). The solvent had no appreciable absorption above 230 nm, so that we could observe not only d–d transition bands (320—840 nm) but also charge-transfer (CT) bands (230—350 nm) of the complexes. Because of the large difference in absorption intensities, however, the CT and d–d wavelength regions were measured by separate experiments. The nickel concentrations were 0.5—1.0 mmol dm^{-3} and the pathlength was 0.5 cm for the CT region, whereas they were 1—25 mmol dm^{-3} and 1.0 cm for the d–d region. The absorbance data at 37 (CT) and 49 (d–d) wavelengths were used for analysis.

Reaction heats were measured with a twin-type calorimeter (Tokyo Riko) at (25±0.0001)°C. An $Ni(BF_4)_2$ solution (1—30 mmol dm^{-3}) was titrated with a 0.2 mol dm^{-3} $(C_2H_5)_4NCl$ solution under nitrogen atmosphere. Heats observed at each titration point ranged from 0.0 to 1.1 J, with a typical uncertainty of ±0.025 J. Heats of dilution were separately measured by titrating a 0.2 mol dm^{-3} $(C_2H_5)_4NBF_4$ solution with the titrant, which were found to be small and used for correction.

Data Analysis. Observed absorbances and reaction heats were analyzed by considering the following complexation equilibria:

$$Ni^{2+} + nCl^- \rightleftarrows [NiCl_n]^{(2-n)+} \quad (1)$$

$$(n = 1, \cdots, N_{\max}).$$

At the ith titration point, total concentrations of nickel and chloride ions, $C_{M,i}$ and $C_{X,i}$, are expressed as

$$C_{M,i} = [M]_i + \Sigma\beta_n[M]_i[X]_i^n, \quad (2)$$

$$C_{X,i} = [X]_i + \Sigma n\beta_n[M]_i[X]_i^n, \quad (3)$$

where $[M]_i$ and $[X]_i$ denote the concentrations of free metal and ligand ions, respectively, and β_n the overall formation constant of $[NiCl_n]^{(2-n)+}$. An absorbance of the ith solution at the jth wavelength, $A_{ij,calcd}$, is calculated from Lambert-Beer's law:

$$A_{ij,calcd} = d(\epsilon_{j0}[M]_i + \Sigma\epsilon_{jn}\beta_n[M]_i[X]_i^n), \quad (4)$$

where d denotes the pathlength, and ϵ_{j0} and ϵ_{jn} are the molar extinction coefficients of Ni^{2+} and $[NiCl_n]^{(2-n)+}$, respectively, at the jth wavelength. Formation constants and molar extinction coefficients were simultaneously determined by minimizing the error-square sum, $U=\Sigma(A_{ij,calcd}-A_{ij,obsd})^2$.

Similarly, a heat of complexation at the ith titration point, $q_{i,calcd}$, is calculated as

$$q_{i,calcd} = -\Sigma\Delta H^\circ_{\beta n}\beta_n([M]_i[X]_i^n V_i - [M]_{i-1}[X]_{i-1}^n V_{i-1}), \quad (5)$$

where $\Delta H^\circ_{\beta n}$ denotes the enthalpy of reaction (1) and V_i the volume of the solution. Formation constants and enthalpies of the complexes were determined by minimizing the error-square sum, $U=\Sigma(q_{i,calcd}-q_{i,obsd})^2$.

Results

Spectrophotometry. Figure 1a shows typical spectral changes with titration in the wavelength region 230—350 nm. Solvated nickel(II) ion had no appreciable absorption in this region, but intense absorption bands grew up as the $(C_2H_5)_4NCl$ solution was added. We analyzed the absorbance data by postulating several sets of plausible complexes (Table 1). Two sets give a relatively small R factor: set (1—4) in which the formation of four successive mononuclear complexes, $[NiCl_n]^{(2-n)+}$ $(n=1—4)$, is considered, and set (1,3, 4) in which only the formation of $[NiCl]^+$, $[NiCl_3]^-$, and $[NiCl_4]^{2-}$ is considered. Other sets such as (2,3,4), (1,2,4), and (1,2,3) give much larger R values (>4%). As set (1—4) results in an appreciably smaller R value (0.45%) than that of set (1,3,4) (0.61%), the formation of the dichloro complex in solution is presumable. Electronic spectra of the individual complexes are shown in Fig. 1b. The molar extinction coefficients for $[NiCl_2]$ have large standard deviations ($3\sigma\approx170$), whereas those for the other three complexes have much smaller uncertainties ($3\sigma<36$).

Figure 2a shows absorption spectra over 320—840 nm. The $Ni(BF_4)_2$ solution exhibited a weak absorption due to d-d transition at 363 nm, and as the chloride concentration increased, the peak position shifted to a longer wavelength (ca. 390 nm). Further addition of Cl^- aroused stronger absorption bands over 550—750 nm. The peaks at 656 and 703 nm are characteristic for tetrahedral $[NiCl_4]^{2-}$ complex.[11,12] Because of the relatively small extinction coefficients, higher metal concentrations were required for these measurements; however, in solutions of $C_M>2.5$ mmol dm^{-3}, yellow precipitates of $NiCl_2\cdot2MeCN$ appeared[13] as C_X/C_M passed 2, and spectral data were not obtainable around this concentration ratio. At $C_X/C_M>3$, the precipitates were again dissolved and completely disappeared, so that the measurement could be continued. In the case of $C_M<2.2$ mmol dm^{-3}, there was no indication of precipitation such as a uniform increase in absorbance or serious deviations from the mass-balance law.

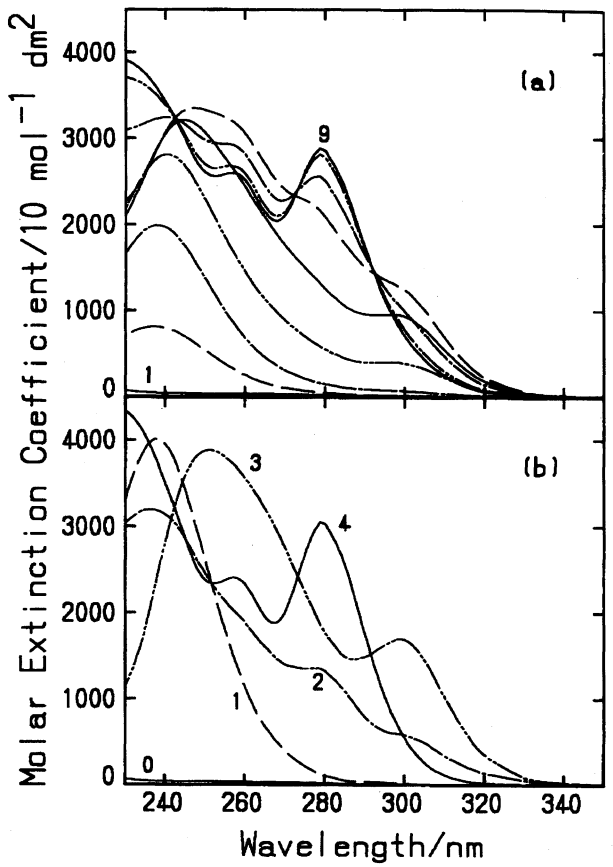

Fig. 1. (a) Typical electronic spectra of nickel(II) chloride MeCN solutions in the wavelength region of 230—350 nm. Apparent extinction coefficients are plotted, i.e., absorbances are normalized with the total metal concentration. The initial metal concentration was $C_{M,init}=0.517$ mmol dm^{-3}, and the C_X/C_M ratio ranged as follows: 0 (line 1), 0.207, 0.622, 1.38, 2.41, 3.79, 5.52, 9.64, 13.8 (line 9). (b) Electronic spectra of individual nickel(II) chloro complexes in MeCN. The numbers represent n within $[NiCl_n]^{(2-n)+}$.

Because of the lack of data due to precipitation and the limited span of the metal concentrations, the least-squares analysis of the d-d spectral data failed to give reliable values for the formation constants. Nevertheless, we could reproduce the d-d data fairly well by using

Table 1. Overall Formation Constants, $\log(\beta_n/\mathrm{mol}^{-n}\,\mathrm{dm}^{3n})$, of $[NiCl_n]^{(2-n)+}$ (n=1—4) Determined by Spectrophotometry (230—350 nm) in Acetonitrile Containing 0.2 mol dm^{-3} $(C_2H_5)_4NBF_4$ at 25°C

	(1—4)	(1,3,4)
$\log \beta_1$	4.86(1)	4.90(2)
$\log \beta_2$	8.61(5)	—
$\log \beta_3$	13.40(3)	13.43(4)
$\log \beta_4$	16.69(3)	16.64(3)
N[a)]	2997	2997
σ_{obsd}[b)]	0.0031	0.0041
R[c)]	0.0045	0.0061

Values in parentheses refer to three standard deviations (3σ) to the final digits. a) Number of data points. b) Estimated standard deviation of the observed absorbances. c) Hamilton R factor.

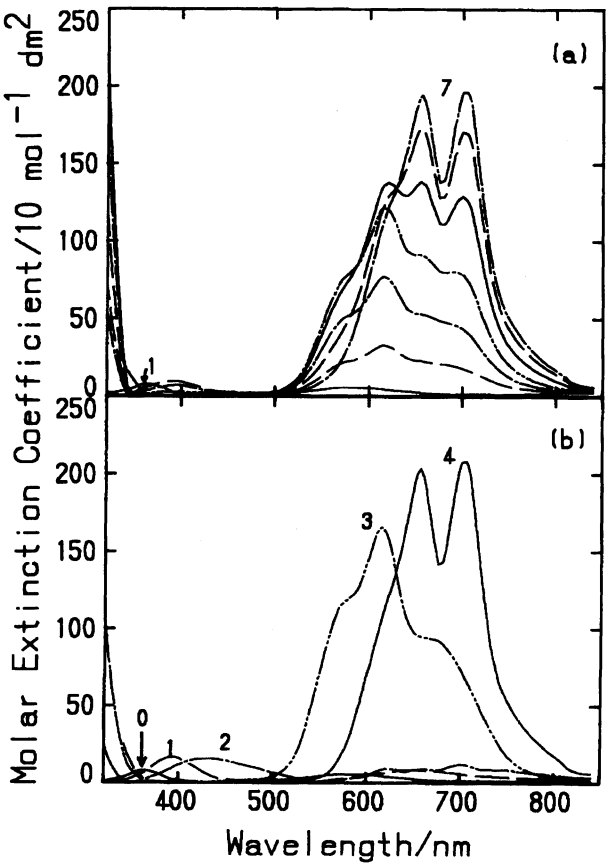

Fig. 2. (a) Typical electronic spectra of nickel(II) chloride MeCN solutions in the wavelength region of 320—840 nm. Absorbances are normalized with the total metal concentration. The initial metal concentration was $C_{M,init}=2.18$ mmol dm^{-3}, and the C_X/C_M ratio ranged as follows: 0 (line 1), 1.18, 1.97, 2.76, 3.55, 4.34, 6.58 (line 7). (b) Electronic spectra of individual nickel(II) chloro complexes in MeCN. The numbers represent n within $[NiCl_n]^{(2-n)+}$.

the formation constants from the CT data (Table 1), with N=3920, σ_{obsd}=0.0024 and R=1.1%. Figure 2b indicates d-d electronic spectra of the individual complexes, which were obtained by using these formation constants. The molar extinction coefficients for the major three complexes are determined with good accuracy ($3\sigma<2$), whereas the minor complex $[NiCl_2]$ has $3\sigma\approx13$.

Calorimetry. Figure 3 shows calorimetric titration curves, in which enthalpies of titration $-q(C_{X,titr}\delta v)^{-1}$ are plotted against C_X/C_M; here the symbol $C_{X,titr}$ represents the total concentration of chloride ion in the titrant, and δv the volume of the titrant added at each titration point. In solutions of $C_M>2.5$ mmol dm^{-3}, heat data around $C_X/C_M\approx2$ were extraordinarily scattered owing to precipitation heats, and omitted from both the figure and the analysis.

The lack of data at $C_X/C_M\approx2$ again prevented us from determining the formation constants by the least-squares analysis of the heat data. Therefore, we determined enthalpies from the data by using the spectrophotometrically obtained formation constants (Table 1). The results are listed in Table 2. Set (1—4) reproduces the observed heats with a tolerable standard deviation, σ_{obsd}=0.05 J (R=17%). The maximum mole fraction of $[NiCl_2]$ in solution is 11% and thus its contribution to the net heats is small, leading to a large uncertainty in $\Delta H^\circ_{\beta2}$, whereas $\Delta H^\circ_{\beta3}$ and $\Delta H^\circ_{\beta4}$ are obtained with a fair accuracy. In fact, set (1,3,4) reproduces the observed heats to the similar extent (σ_{obsd}=0.06 J, R=19%), and the enthalpies for the other three complexes are practically unchanged in both sets (Table 2).

The solid lines in Fig. 3 were calculated with the constants obtained for set (1—4). It is noted that systematic deviations at $C_X/C_M\approx2$ are apparent even at lower metal concentrations, which might be due to colloidal precipitation. These deviations ($q_{i,calcd}-q_{i,obsd}$) are, however, actually rather small (<0.1 J) and less important in the analysis; in the figure, deviations are emphasized for the data with small δv, owing to the normalization of the heats into the form $-q(C_{X,titr}\delta v)^{-1}$. They are more likely to be due to other experimental errors (concentrations, volumes, residual water, and dilution heat correction). We numerically examined a possible influence on the obtained enthalpies, by eliminating the data points at C_X/C_M=1.5—3.5 and analyzing the rest of the data, which gave similar enthalpy values within 3σ.

Discussion

Electronic Spectra and Coordination Structures. In the d-d wavelength region, the solvated Ni^{2+} ion exhibits a weak absorption peak at 363 nm and a very broad band around 580 nm (Fig. 2b), which are typical for the octahedral environment around Ni center.[11] It is consistent with the reported structure of a solvate crystal $[Ni(MeCN)_6]$ $[ZnCl_4]$, in which the solvated nickel ion forms a nearly regular octahedron, with the mean Ni–N–C angles of 172°.[14] The d-d spectrum of the monochloro complex is very similar to that of Ni^{2+} except for the peak positions, which are shifted to a

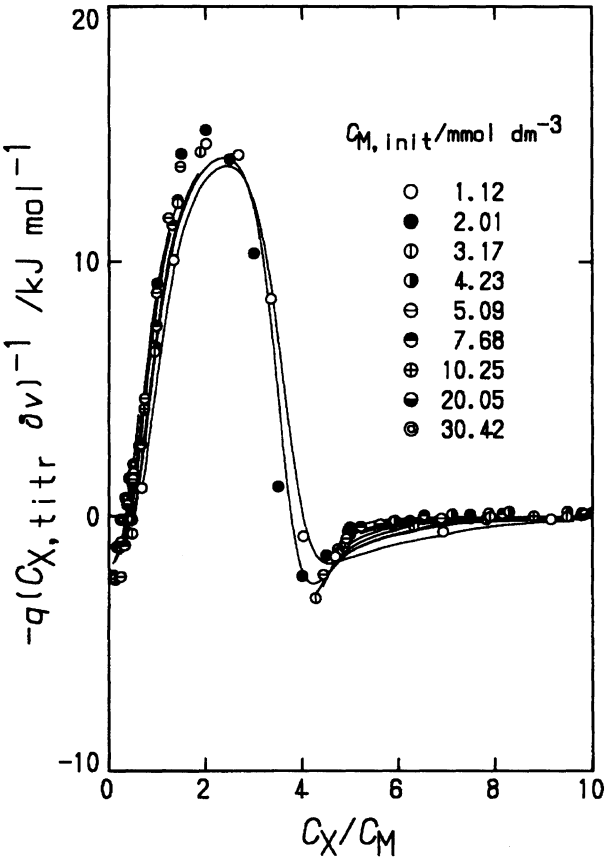

Fig. 3. Calorimetric titration curves of nickel(II) chloride MeCN solutions. Initial concentrations of metal ion are displayed in the figure. The solid lines show the theoretical curves calculated by using the constants for Set (1—4) in Tables 1 and 2.

Table 2. Overall Enthalpies, $\Delta H^\circ_{\beta n}$/kJ mol^{-1}, of $[NiCl_n]^{(2-n)+}$ (n=1—4) Determined by Calorimetry in Acetonitrile Containing 0.2 mol dm^{-3} $(C_2H_5)_4NBF_4$ at 25°C

	(1—4)	(1,3,4)
$\Delta H^\circ_{\beta 1}$	−2.0(7)	−1.6(5)
$\Delta H^\circ_{\beta 2}$	6(9)	—
$\Delta H^\circ_{\beta 3}$	37(3)	33(2)
$\Delta H^\circ_{\beta 4}$	27(3)	25(3)
N[a]	101	101
σ_{obsd}[b]	0.052	0.057
R[c]	0.17	0.19

Values in parentheses refer to three standard deviations (3σ) to the final digits. Enthalpies were evaluated by using the formation constants obtained from the CT spectra (Table 1). a) Number of data points. b) Estimated standard deviation of the observed quantity (heats/J). c) Hamilton R factor.

longer wavelength in accordance with the spectrochemical series of the ligating atoms (N>Cl$^-$). The spectrum of the dichloro complex is again similar and further red-shifted, even if we consider the large uncertainty of the spectrum. Therefore, we may conclude that these three species have octahedral coordination structures, which are formulated as $[Ni(MeCN)_6]^{2+}$, $[NiCl(MeCN)_5]^+$, and $[NiCl_2(MeCN)_4]$. On the other hand, the tri- and tetrachloro complexes have much more intense absorption bands over 600—700 nm, which are clearly diagnostic of tetrahedral structures $[NiCl_3(MeCN)]^-$ and $[NiCl_4]^{2-}$.[11,12]

The same conclusion has been drawn for the nickel(II) chloro complexes in DMF solution, i.e., the structural transition from octahedral to tetrahedral occurs on the formation of $[NiCl_3]^-$ both in MeCN and in DMF.[15] Comparison of the d-d spectra in both solvents shows that the energy of the spin-allowed transition $^3A_{2g}\rightarrow{}^3T_{1g}(P)$[11] of solvated Ni^{2+} is higher in MeCN, in accord with the stronger ligand-field of MeCN than that of DMF. The solvatochromism becomes less significant in the complexes, as more solvent molecules are replaced by Cl$^-$. The spectrum of $[NiCl_4]^{2-}$ in MeCN is almost identical to those in DMF,[15] dimethyl sulfoxide (DMSO),[16] and *N,N*-dimethylacetamide (DMA),[17] which is consistent with the absence of solvent molecules in the first coordination sphere.

A drastic change by complexation is also seen in the wavelength region 230—350 nm (Fig. 1b). In contrast to the $[Ni(MeCN)_6]^{2+}$ ion, the complexes exhibit intense absorption bands due to chlorine-to-nickel charge transfer (LMCT) transitions in this region. The spectra of the mono- and dichloro complexes are primarily composed of a single transition at ca. 240 nm, which may be assigned to $\pi(L)\rightarrow 2e_g(\sigma^*)$ transition on the basis of O_h symmetry.[11] The latter spectrum has a long tail over 260—320 nm, but the large uncer-

Table 3. Thermodynamic Quantities, log (K_n/mol^{-1} dm^3), ΔG°_n/kJ mol^{-1}, ΔH°_n/kJ mol^{-1}, and ΔS°_n/J K^{-1} mol^{-1}, for the stepwise formation of $[NiCl_n]^{(2-n)+}$ in acetonitrile (MeCN) and *N,N*-dimethylformamide (DMF) at 25°C

	MeCN	DMF[a]
log K_1	4.86(1)	2.85
log K_2	3.75(5)	0.91
log K_3	4.79(5)	1.77
log K_4	3.29(1)	1.87
ΔG°_1	−27.71(7)	−16.3
ΔG°_2	−21.4(3)	−5.2
ΔG°_3	−27.3(3)	−10.1
ΔG°_4	−18.77(6)	−10.7
ΔH°_1	−2.0(7)	8.6
ΔH°_2	8(10)	19.1
ΔH°_3	30(12)	62.9
ΔH°_4	−10(2)	−13.4
ΔS°_1	87(2)	84
ΔS°_2	100(32)	82
ΔS°_3	193(39)	245
ΔS°_4	30(8)	−9

Values in parentheses refer to three standard deviations (3σ) to the final digits. a) 0.4 mol dm^{-3} $(C_2H_5)_4NClO_4$ (Ref. 15).

Table 4. Overall Thermodynamic Quantities, $\Delta G^\circ_{\beta 4}$/kJ mol^{-1}, $\Delta H^\circ_{\beta 4}$/kJ mol^{-1}, and $\Delta S^\circ_{\beta 4}$/J K^{-1} mol^{-1}, for the formation of $[MCl_4]^{2-}$ in acetonitrile (MeCN) and *N,N*-dimethylformamide (DMF) at 25°C (M=Ni, Cu, and Zn)

	MeCN			DMF		
	Ni	Cu[a]	Zn[b]	Ni[c]	Cu[d]	Zn[c]
$\Delta G^\circ_{\beta 4}$	−95.2(2)	−145.2	−131.3(9)	−42(1)	−96.2	−110(4)
$\Delta H^\circ_{\beta 4}$	27(3)	−55.4	−45(2)	77(2)	19.2	−9.4(6)
$\Delta S^\circ_{\beta 4}$	409(11)	301	289(6)	401(9)	388	338(15)

Values in parentheses refer to three standard deviations (3σ) to the final digits. a) 0.1 mol dm^{-3} $(C_2H_5)_4NClO_4$ (Ref. 3). b) 0.1 mol dm^{-3} $C_5H_6NCF_3SO_3$ (Ref. 5). c) 0.4 mol dm^{-3} $(C_2H_5)_4NClO_4$ (Ref. 15). d) 0.2 mol dm^{-3} $(C_2H_5)_4NClO_4$ (Ref. 4).

tainty hinders interpretation in detail. The tri- and tetrachloro complexes have several transitions in this region; for $[NiCl_4]^{2-}$, agreement with the published spectra is excellent, and assignment can be made as $t_1(\pi,\text{non-bonding}) \rightarrow 4t_2(\sigma^*,\pi^*)$ for the transitions at 257 and 280 nm, and $3t_2(\pi) \rightarrow 4t_2(\sigma^*,\pi^*)$ for the transition at ca. 230 nm.[18—20]

It has been argued that octahedral nickel(II) species exhibit Ni-halogen LMCT bands at higher energies than analogous tetrahedral systems.[11] This tendency is also seen in Fig. 1b, i.e., the lowest CT transition of the octahedral mono- and dichloro complexes is located at an energy which is ca. 7700 cm^{-1} higher than that of the tetrahedral tri- and tetrachloro complexes. Oppositely to the d-d spectra (Fig. 2b), the CT spectrum of $[NiCl_4]^{2-}$ is blue-shifted as compared with $[NiCl_3(MeCN)]^-$, suggesting that the replacement of MeCN by Cl^- in the tetrahedral geometry may raise the net energy of the metal acceptor orbital (t_2), even though the ligand field splitting decreases.

Thermodynamics of Complexation. Thermodynamic parameters, log (K_n/mol^{-1} dm^3), ΔG°_n/kJ mol^{-1}, ΔH°_n/kJ mol^{-1}, and ΔS°_n/J K^{-1} mol^{-1}, for the stepwise formation of $[NiCl_n]^{(2-n)+}$ in MeCN and in DMF[15] are summarized in Table 3. The obtained log K_4 value (3.29) is in rough agreement with the previously estimated value (3.05).[21] Distribution of the nickel complexes in MeCN and in DMF is depicted in Fig. 4.

The overall formation of the tetrachloronickelate-(II) complex is much weaker than the Cu^{II} and Zn^{II} analogues in both solvents (Table 4). The weak formation of the Ni^{II} complex is attributable to the marked endothermicity of the reaction in both solvents; the corresponding entropies are rather favorable for Ni^{II}, but they are overcome by the much larger enthalpy difference. Since the coordination structure changes from octahedral to tetrahedral through this reaction, ligand field stabilization energies (LFSE) are expected to play an important role. The LFSE values of the solvated Ni^{II} ions and the tetrachloro complex may be estimated from D_q values as follows: $[Ni(MeCN)_6]^{2+}$, LFSE=151 kJ mol^{-1} (D_q=1050 cm^{-1});[22] $[Ni(DMF)_6]^{2+}$, 122 (850);[23] $[NiCl_4]^{2-}$, 33.9

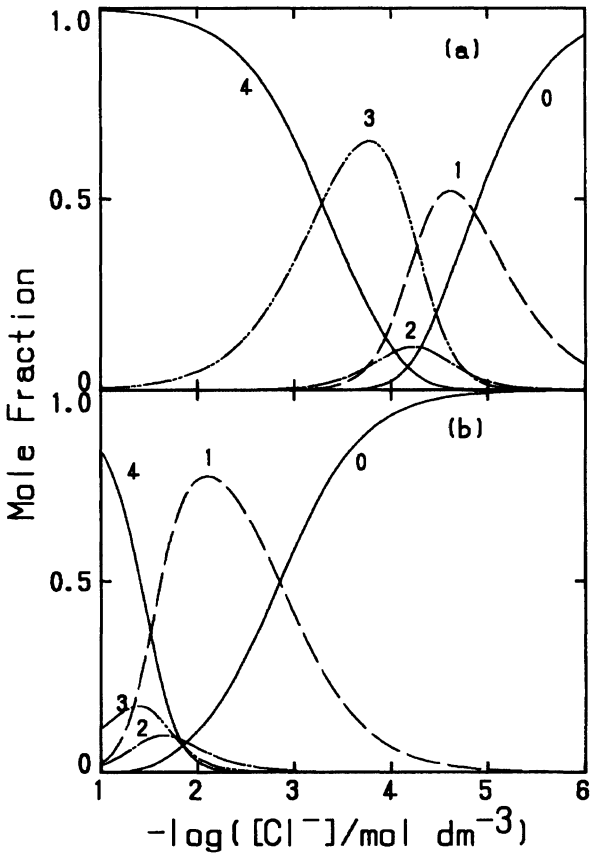

Fig. 4. Distribution of the nickel(II) chloro complexes in MeCN (a) and in DMF (b). The numbers represent n within $[NiCl_n]^{(2-n)+}$.

(354).[24] The LFSE energies for Cu^{II} are difficult to estimate because of the Jahn-Teller effect. The difference between the LFSE energies of solvated Ni^{2+} and that of $[NiCl_4]^{2-}$ is thus 117 kJ mol^{-1} in MeCN and 88 kJ mol^{-1} in DMF, which may be compared with $\Delta H^\circ_{\beta 4}(Ni^{II}) - \Delta H^\circ_{\beta 4}(Zn^{II}) = 72$ (in MeCN) and 86 (in DMF). Accordingly, the instability of the Ni^{II} complex may be primarily ascribed to the loss of LFSE due to the structural transition from octahedral to tetrahedral geometry.

Complexation is strongly enhanced in MeCN than in DMF, for all metal ions included in Table 4. This is clearly due to the exothermicity of the complexation

reactions in MeCN compared with in DMF. Because complexation accompanies desolvation of the metal ion, it is reasonable that the reaction is more exothermic in MeCN, where the metal ion is more weakly solvated. Indeed, enthalpies of transfer of these ions from DMF to MeCN can be evaluated as 66.0 kJ mol^{-1} (Ni^{2+}), 80.1 (Cu^{2+}), and 85.9 (Zn^{2+}),[3,22,25] which indicates extensive destabilization of the solvated ions in MeCN. The corresponding entropies, however, seem to be less sensitive to the relative strength of metal-solvent bonds; rather, it may reflect extensive production of freedom in motion of solvent molecules released by desolvation.[3,4,16,26] In this context, X-ray diffraction studies on liquid structures of MeCN and DMF revealed disordered arrangements of solvent molecules beyond the nearest neighbors, although dipole–dipole interactions are noticeable between adjacent MeCN molecules.[27] This suggests that bulk phase of both MeCN and DMF are fairly disordered and randomly configured, being consistent with the alikeness of the complexation entropies in these solvents.

This work has been financially supported by Grant-in-Aid for Scientific Research No. 04640572 and for Scientific Research on Priority Area No. 04215209 from the Ministry of Education, Science and Culture.

References

1) J. A. Riddick, W. B. Bunger, and T. K. Sakano, "Organic Solvents," 4th ed, Wiley-Interscience, New York (1986).
2) V. Gutmann, "The Donor–Acceptor Approach to Molecular Interactions," Plenum, New York and London (1978).
3) S. Ishiguro, B. G. Jeliazkova, and H. Ohtaki, *Bull. Chem. Soc. Jpn.*, **58**, 1749 (1985).
4) S. Ishiguro, B. G. Jeliazkova, and H. Ohtaki, *Bull. Chem. Soc. Jpn.*, **58**, 1143 (1985).
5) I. Persson, K. C. Dash, and Y. Kinjo, *Acta Chem. Scand.*, **44**, 433 (1990).
6) R. C. Kapoor and J. Kishan, *Rev. Anal. Chem.*, **1981**, 257.
7) B. J. Hathaway and A. E. Underhill, *J. Chem. Soc.*, **1960**, 3705.
8) B. J. Hathaway, D. G. Holah, and A. E. Underhill, *J. Chem. Soc.*, **1962**, 2444.
9) H. Flaschka and H. Abdine, *Chemist-Analyst*, **45**, 58 (1956).
10) D. T. Sawyer and J. L. Roberts, Jr., "Experimental Electrochemistry for Chemists, " Wiley-Interscience, New York (1974).
11) A. P. B. Lever, "Inorganic Electronic Spectroscopy, " 2nd ed, Elsevier, Amsterdam (1984).
12) C. P. Nash and M. S. Jenkins, *J. Phys. Chem.*, **68**, 356 (1964).
13) B. J. Hathaway and D. G. Holah, *J. Chem. Soc.*, **1962**, 2400.
14) I. Søtofte, R. G. Hazell, and S. E. Rasmussen, *Acta. Crystallogr., Sect. B*, **32**, 1692 (1976).
15) S. Ishiguro, K. Ozutsumi, and H. Ohtaki, *Bull. Chem. Soc. Jpn.*, **60**, 531 (1987).
16) H. Suzuki, S. Ishiguro, and H. Ohtaki, *J. Chem. Soc., Faraday Trans.*, **86**, 2179 (1990).
17) H. Suzuki and S. Ishiguro, *Inorg. Chem.*, **31**, 4178 (1992).
18) P. Day and C. K. Jørgensen, *J. Chem. Soc.*, **1964**, 6226.
19) B. D. Bird and P. Day, *J. Chem. Phys.*, **49**, 392 (1968).
20) A. G. Coutts and P. Day, *Phys. Status Solidi B*, **88**, 767 (1978).
21) T. W. Gilbert and L. Newman, *Inorg. Chem.*, **9**, 1705 (1970).
22) W. Libuś, M. Mecik, and H. Strzelecki, *J. Solution Chem.*, **9**, 723 (1980).
23) R. S. Drago, D. W. Meek, M. D. Joesten, and L. LaRoche, *Inorg. Chem.*, **2**, 124 (1963).
24) G. P. Smith, C. H. Liu, and T. R. Griffiths, *J. Am. Chem. Soc.*, **86**, 4796 (1964).
25) M. Mecik and A. Chudziak, *J. Solution Chem.*, **14**, 653 (1985).
26) S. Ahrland, *Pure Appl. Chem.*, **51**, 2019 (1979).
27) T. Radnai, S. Itoh, and H. Ohtaki, *Bull. Chem. Soc. Jpn.*, **61**, 3845 (1988).